

## Chiroselective Assembly of a Chiral Porphyrin–Fullerene Dyad: Photoconductive Nanofiber with a Top-Class Ambipolar Charge-Carrier Mobility

Yumi Hizume,<sup>†</sup> Kentaro Tashiro,<sup>\*,‡</sup> Richard Charvet,<sup>\*,‡</sup> Yohei Yamamoto,<sup>§</sup> Akinori Saeki,<sup>||</sup> Shu Seki,<sup>||</sup> and Takuzo Aida<sup>\*,†,§</sup>

School of Engineering, The University of Tokyo, 7-3-1 Hongo, Bunkyo-ku, Tokyo 113-8656, Japan, ERATO-SORST Nanospace Project, Japan Science and Technology Agency (JST), National Museum of Emerging Science and Innovation, 2-41 Aomi, Koto-ku, Tokyo 135-0064, Japan, National Institute for Materials Science, 1-1 Namiki, Tsukuba 305-0044, Japan, and Department of Applied Chemistry, Osaka University, 2-1 Yamadaoka, Suita, Osaka 565-0871, Japan

Received February 19, 2010; E-mail: aida@macro.t.u-tokyo.ac.jp; tashiro.kentaro@nims.go.jp; racharvet@yahoo.com

Photoconductive 1D nanostructures with a supramolecular p/n-heterojunction (SHJ) have received attention because of their potential utility for photovoltaics.<sup>1</sup> However, examples are still very limited. In pioneering work, Würthner et al. reported that a hydrogen-bonded donor–acceptor–donor (D-A-D) triad consisting of oligo(*p*-phenylene vinylene) (D) and perylene diimide (A) self-assembles into a photoconductive nanofiber.<sup>1a,b</sup> Meanwhile, we found that an amphiphilic dyad consisting of hexa-*peri*-hexabenzocoronene (HBC) and trinitrofluorenone (TNF) self-assembles into a photoconductive coaxial nanotube, whose graphite-like wall is laminated by an electron-accepting TNF layer.<sup>1c</sup> This strategy was extended to the fabrication of a photovoltaic nanotube from an amphiphilic HBC–fullerene dyad.<sup>1e</sup> In these cases, intermolecular charge-transfer (CT) complexation between the D and A units is likely suppressed by the amphiphilic molecular design.<sup>2</sup> Here we report self-assembly of an amphiphilic porphyrin–fullerene dyad (**1**, Figure 1a), which was designed to form a photoconductive 1D SHJ nanostructure with an enhanced absorptivity for visible light.<sup>3</sup> Dyad **1** is a modified version of our previously reported porphyrin–fullerene dyad with an ester bridge, which stacks unfavorably via a CT interaction to give multilamellar vesicles.<sup>4</sup> With a view to change the self-assembling mode, the modified dyad carries a smaller hydrophilic wedge than the previous one and utilizes a triazole unit for bridging the D and A components. However, as described below, dyad **1** again self-assembled into a spherical object. Furthermore, the *I*–*V* profile of its cast film hardly showed a photoconductivity. Note that dyad **1** is chiral with a stereogenic center in its fullerene unit. Hence, we decided to take a chance on the possibility that enantiopure **1** might self-assemble differently from its racemate,<sup>5</sup> and finally we obtained a photoconductive nanofiber with the desired D/A geometry. Moreover, its film sample showed a top-class ambipolar charge-carrier mobility.

Compound **1** was synthesized by coupling an azide-appended zinc porphyrin with a fullerene having an alkyne unit, followed by acidic demetalation of the porphyrin moiety, and unambiguously characterized by <sup>1</sup>H NMR and MALDI-TOF-MS analyses.<sup>6</sup> Dyad **1** was highly soluble in CH<sub>2</sub>Cl<sub>2</sub>, giving a red solution with a Soret band at 410 nm (Figure 1b-i).<sup>6</sup> To obtain enantiopure **1**, a Prato-type chiral fullerene<sup>7</sup> with a Me<sub>3</sub>Si-protected alkyne was optically resolved by chiral HPLC.<sup>6</sup> The enantiomers of **1**, thus obtained, showed mirror-image circular dichroism (CD) spectra of one another

with positive ((+)-**1**, Figure 1c-i) and negative ((-)-**1**, Figure 1c-ii) Cotton effects at 430 nm.

When MeOH (1.5 mL) was slowly added onto a CH<sub>2</sub>Cl<sub>2</sub> (0.5 mL) solution of racemic **1** ((±)-**1**, 0.8 mM) and the mixture was allowed to stand for 2 days at 25 °C, a yellowish-brown-colored suspension resulted.<sup>6</sup> The absorption spectrum displayed a broad, red-shifted Soret band centered at 450 nm (Figure 1b-ii). Scanning electron microscopy (SEM) of a cast film of the suspension visualized uniformly sized spheres with an average diameter of 300 nm (Figure 1d). These spectral and morphological aspects resemble those observed for the previously reported spherical assembly.<sup>4</sup> We were disappointed with this result, since spherical assemblies are much less promising than 1D assemblies for long-range charge-carrier transport. However, quite interestingly, when enantiopure (+)-**1** was allowed to self-assemble under identical conditions in CH<sub>2</sub>Cl<sub>2</sub>/MeOH, bundles of very long nanofibers (up to 10 μm) formed (Figure 1e). The absorption spectrum of the resulting suspension showed just a broad Soret band with a small red-shifted shoulder at 440 nm (Figure 1b-iii), quite different from that observed for the spherical assembly from (±)-**1**. Such an absorption spectral

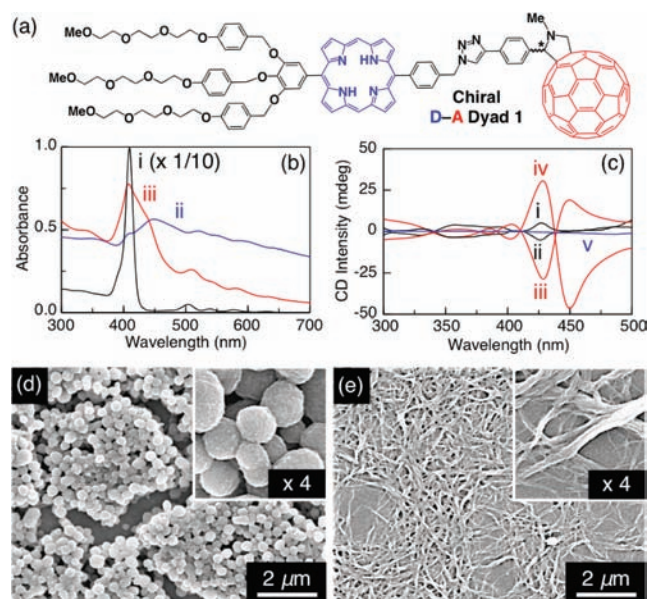


**Figure 1.** (a) Molecular structure of **1**. (b) Absorption spectra of (i) a CH<sub>2</sub>Cl<sub>2</sub> solution of (±)-**1** and CH<sub>2</sub>Cl<sub>2</sub>/MeOH suspensions of assembled (ii) (±)-**1** and (iii) (+)-**1** at 25 °C. (c) CD spectra of CH<sub>2</sub>Cl<sub>2</sub> solutions of (i) (+)-**1** and (ii) (-)-**1** and CH<sub>2</sub>Cl<sub>2</sub>/MeOH suspensions of assembled (iii) (+)-**1**, (iv) (-)-**1**, and (v) (±)-**1** at 25 °C. SEM micrographs of cast films of assembled (d) (±)-**1** and (e) (+)-**1**.

<sup>†</sup> The University of Tokyo.

<sup>‡</sup> National Institute for Materials Science.

<sup>§</sup> ERATO-SORST Nanospace Project.

<sup>||</sup> Osaka University.

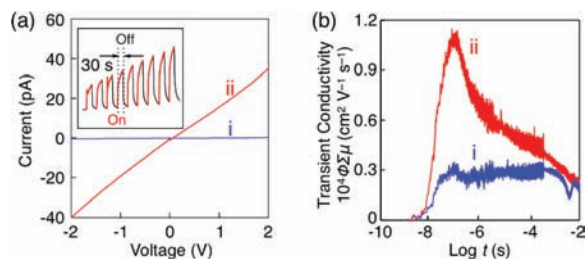


**Figure 2.** (a)  $I$ – $V$  profiles at 25 °C of assembled (i) (±)-**1** and (ii) (+)-**1** (inset: switching response of photocurrent for assembled (+)-**1**) upon photoexcitation at  $\lambda = 300$ – $650$  nm and (b) their FP-TRMC profiles at 16 °C upon photoexcitation with a 355-nm laser pulse.

profile is a good sign for D/A-SHJ, since it is typical of porphyrin homoaggregates.<sup>8</sup> The suspension displayed a highly enhanced split Cotton effect in the red-shifted shoulder region of the Soret band of the porphyrin (Figure 1c-iii), indicating that the assembled porphyrin units are efficiently coupled excitonically. As expected, when (–)-**1** was used for the assembly,<sup>6</sup> an opposite-signed split Cotton effect resulted (Figure 1c-iv). Out of curiosity, we attempted the assembly of a 3:1 mixture of (+)-**1** and (–)-**1** (50% ee) under conditions identical to those described above, where only spherical objects resulted (Figure S5a, Supporting Information). The observed CD spectrum was rather similar to that of unassembled (+)-**1** in  $\text{CH}_2\text{Cl}_2$ .<sup>6</sup> Although many chiral molecules have been reported whose enantiomers and racemates self-assemble differently from one another,<sup>5a,c</sup> those giving rise to quite different morphologies such as spheres and fibers are very rare.<sup>5b,d</sup>

The  $\text{CH}_2\text{Cl}_2/\text{MeOH}$  suspensions of the nanofibers and spheres of **1** were cast onto a Si/SiO<sub>2</sub> substrate equipped with micrometer-gap Au/Ti electrodes, and their photoconducting properties were evaluated by a two-probe method.<sup>6</sup> When the nanofiber sample from (+)-**1** was exposed to xenon light ( $\lambda = 300$ – $650$  nm), a photocurrent emerged in the resulting  $I$ – $V$  profile (Figure 2a-ii) and turned off as soon as the photoirradiation was stopped (inset; switching response). Upon photoexcitation with a 355-nm laser pulse, the nanofiber sample, sandwiched by an Al substrate and an ITO electrode, displayed a distinct transient photocurrent in its time-of-flight (TOF) profile both under positive and negative electric fields (Figure S6a, Supporting Information), demonstrating that the nanofiber bears an ambipolar charge-transporting character.<sup>6</sup> It is noteworthy that its electron ( $\mu_e$ ) and hole ( $\mu_h$ ) mobilities in TOF (Figure S6c) were remarkably high and even better than those reported for top-class organic materials with a D/A heterojunction.<sup>9</sup> For example,  $\mu_e$  and  $\mu_h$  under an electric field of  $1 \times 10^{-4}$  V cm<sup>-1</sup> are 0.08 and 0.06 cm<sup>2</sup> V<sup>-1</sup> s<sup>-1</sup>, respectively. Mobilities  $\mu_e$  and  $\mu_h$  under zero electric field, as extrapolated from their dependencies on the applied electric field, were 0.14 and 0.10 cm<sup>2</sup> V<sup>-1</sup> s<sup>-1</sup>, respectively.<sup>6</sup> In sharp contrast, a cast film of the spherical assembly from (±)-**1** hardly showed a photocurrent on the micrometer-gap electrodes (Figure 2a-i). Furthermore, its TOF profile showed no detectable electron mobility and only a very small hole mobility ( $1.5 \times 10^{-4}$  cm<sup>2</sup> V<sup>-1</sup> s<sup>-1</sup> under zero electric field; Figure S6d).<sup>6</sup> With these contrasting macroscopic transport properties in mind, we measured flash-photolysis time-resolved microwave conductivities (FP-TRMC) of the samples. This electrodeless method allows for evaluating short-range (intrinsic) transient conductivities of

materials.<sup>10</sup> Upon exposure to a 355-nm laser pulse at 16 °C, the nanofiber and sphere samples showed maximum transient conductivities of  $1.2 \times 10^{-4}$  and  $0.3 \times 10^{-4}$  cm<sup>2</sup> V<sup>-1</sup> s<sup>-1</sup> (Figure 2b), respectively. Since their quantum yields  $\phi$ , necessary for evaluating the charge-carrier mobilities, were unavailable spectroscopically due to light scattering, they were estimated on the basis of the integrated currents in TOF under zero electric field (Figure S7, Supporting Information).<sup>6</sup> Consequently, we found that the nanofiber is 5.6 times less efficient than the sphere at photogeneration of charge carriers. By using these quantum yields,<sup>10</sup> the intrinsic charge-carrier mobility in the nanofiber was estimated to be 1 order of magnitude greater than that in the sphere.<sup>6</sup>

In conclusion, through a study on the self-assembly of a chiral amphiphilic D–A dyad (**1**), we found that chirality plays a decisive role in generating a supramolecular architecture capable of efficiently transporting charge carriers not only for a short distance but also over a much larger length scale. We also highlight that the photoconductive nanofiber obtained from enantiopure **1** displays a top-class ambipolar charge-carrier mobility ( $\sim 10^{-1}$  cm<sup>2</sup> V<sup>-1</sup> s<sup>-1</sup>), which is far better than that of the spherical assembly from racemic **1**.

**Acknowledgment.** This work was partially supported by a Grant-in-Aid for Scientific Research on Innovative Areas (No. 20108001, “pi-Space”) from MEXT, Japan.

**Supporting Information Available:** Synthesis and characterization of **1**, SEM, spectral, and TOF profiles of assembled **1**. This material is available free of charge via the Internet at <http://pubs.acs.org>.

## References

- (1) (a) Würthner, F.; Chen, Z.; Hoeben, F. J. M.; Osswald, P.; You, C.-C.; Jonkheijm, P.; van Herrikhuizen, J.; Schenning, A. P. H. J.; van der Schoot, P. P. A. M.; Meijer, E. W.; Beckers, E. H. A.; Meskers, S. C. J.; Janssen, R. A. J. *J. Am. Chem. Soc.* **2004**, *126*, 10611. (b) Jonkheijm, P.; Stutzmann, N.; Chen, Z.; de Leeuw, D. M.; Meijer, E. W.; Schenning, A. P. H. J.; Würthner, F. *J. Am. Chem. Soc.* **2006**, *128*, 9535. (c) Yamamoto, Y.; Fukushima, T.; Suna, Y.; Ishii, N.; Saeki, A.; Seki, S.; Tagawa, S.; Taniguchi, M.; Kawai, T.; Aida, T. *Science* **2006**, *314*, 1761. (d) Sisson, A. L.; Sakai, N.; Banerji, N.; Fürstenberg, A.; Vauthey, E.; Matile, S. *Angew. Chem., Int. Ed.* **2008**, *47*, 3727. (e) Yamamoto, Y.; Zhang, G.; Jin, W.; Fukushima, T.; Ishii, N.; Saeki, A.; Seki, S.; Tagawa, S.; Minari, T.; Tsukagoshi, K.; Aida, T. *Proc. Natl. Acad. Sci. U.S.A.* **2009**, *106*, 21051.
- (2) (a) Li, W.-S.; Yamamoto, Y.; Fukushima, T.; Saeki, A.; Seki, S.; Tagawa, S.; Masunaga, H.; Sasaki, S.; Takata, M.; Aida, T. *J. Am. Chem. Soc.* **2008**, *130*, 8886. (b) Sakurai, T.; Shi, K.; Sato, H.; Tashiro, K.; Osuka, A.; Saeki, A.; Seki, S.; Tagawa, S.; Sasaki, S.; Masunaga, H.; Osaka, K.; Takata, M.; Aida, T. *J. Am. Chem. Soc.* **2008**, *130*, 13812.
- (3) (a) Gust, D.; Moore, T. A. *Science* **1989**, *244*, 35. (b) Guldi, D. M.; Imahori, H. *J. Porphyrins Phthalocyanines* **2004**, *8*, 976.
- (4) Charvet, R.; Jiang, D.-L.; Aida, T. *Chem. Commun.* **2004**, 2664.
- (5) (a) Oda, R.; Huc, I.; Schmutz, M.; Candau, S. J.; MacKintosh, F. C. *Nature* **1999**, *399*, 566. (b) Moreau, J. J. E.; Vellutini, L.; Man, M. W. C.; Bied, C. *Chem.–Eur. J.* **2003**, *9*, 1594. (c) Estroff, L. A.; Hamilton, A. D. *Biomater. Rev.* **2004**, *104*, 1201. (d) Koga, T.; Matsuoka, M.; Higashi, N. *J. Am. Chem. Soc.* **2005**, *127*, 17596.
- (6) See Supporting Information.
- (7) Prato, M.; Maggini, M. *Acc. Chem. Res.* **1998**, *31*, 519.
- (8) (a) Barber, D. C.; Freitag-Beeston, R. A.; Whitten, D. G. *J. Phys. Chem.* **1991**, *95*, 4074. (b) Kano, K.; Fukuda, K.; Wakami, H.; Nishiyabu, R.; Pasternack, R. F. *J. Am. Chem. Soc.* **2000**, *122*, 7494.
- (9) (a) Shi, Q.; Hou, Y.; Jin, H.; Li, Y. *J. Appl. Phys.* **2007**, *102*, 073108. (b) Ballantyne, A. M.; Chen, L.; Dane, J.; Hammant, T.; Braun, F. M.; Heeney, M.; Duffy, W.; McCulloch, I.; Bradley, D. D. C.; Nelson, J. *Adv. Funct. Mater.* **2008**, *18*, 2373. (c) Charvet, R.; Acharya, S.; Hill, J. P.; Akada, M.; Liao, M.; Seki, S.; Honsho, Y.; Saeki, A.; Ariga, K. *J. Am. Chem. Soc.* **2009**, *131*, 18030.
- (10) Saeki, A.; Seki, S.; Koizumi, Y.; Sunagawa, T.; Ushida, K.; Tagawa, S. *J. Phys. Chem. B* **2005**, *109*, 10015.

JA1014713